JOURNAL OF
Materials
CHEMISTRY

Synthesis and characterization of trialkoxysilane-capped poly(methyl methacrylate)–titania hybrid optical thin films

Wen-Chang Chen,*[a] Shu-Jen Lee,[a] Long-Hua Lee[a] and Jen-Lien Lin[b]

[a] *Department of Chemical Engineering, National Taiwan University, Taipei, Taiwan. E-mail: chenwc@ms.cc.ntu.edu.tw*
[b] *Union Chemical Laboratories, Industrial Technology Research Institute, Hsinchu, Taiwan*

Received 29th July 1999, Accepted 24th September 1999

A series of trialkoxysilane-capped PMMA–titania hybrid optical thin films has been prepared by an *in situ* sol–gel process combined with spin coating and multi-step baking. The used acrylic monomers were methyl methacrylate (MMA) and 3-(trimethoxysilyl)propyl methacrylate (MSMA). Titanium(IV) *n*-butoxide was used for the preparation of the titania network. FTIR results indicate successful bonding between the organic and inorganic moieties. A DSC study suggests a good dispersion of the PMMA segment in the titania network while an AFM study suggests that the prepared hybrid thin films have superior smoothness in comparison to the parent titania thin film. The dispersion of the refractive index and extinction coefficient in the wavelength range 190–900 nm was studied. Variation of the titania content not only tunes the refractive index but also the position of absorption maximum. Off-resonant refractive indices of the prepared hybrid thin films were in the range 1.505–1.553, which linearly increased with the titania content. Furthermore, the hybrid polymer films have abbe numbers (ν) all >30. The shift of the absorption maximum of the prepared hybrid thin films can be correlated with the titania content. The prepared hybrid films show very high optical transparency in the visible region. These results suggest that such hybrid films have potential applications for optical devices.

Introduction

Scientific interest in the preparation of organic–inorganic hybrid materials processed from sol–gel techniques remains very high. Molecular design of the organic and inorganic segments has produced new materials with novel physical and chemical properties.[1,2] New electronic and optical materials based on such kinds of hybrid materials have been extensively reported, and have found applications in areas such as contact lenses,[3] high refractive index materials,[4,5] waveguide materials,[6] optical coatings,[7] nonlinear optical materials,[8] photochromic materials[9] and optical devices.[10]

One of the major challenges for the preparation of the hybrid materials is how to control the phase separation between the organic and inorganic moieties. The phase behavior of the hybrid materials is affected by the interaction between the organic segment and the inorganic network. Hydrogen bonding or covalent bonding is usually used to prevent phase separation.[1] Wilkes and coworkers successfully prepared triethoxysilane capped polymer–titania hybrid materials containing poly(arylene ether ketone)s,[4] poly(arylene ether sulfone)s,[4] and poly(tetramethylene oxide)s.[11] Huang and Qiu used a trialkoxysilane-capped methacrylate to prepare acrylate–silica hybrid materials. They obtained hybrid materials with a strong chemical bonding between the PMMA segment and the silica network and thus no phase separation occurred.[12] Zhang *et al.* prepared poly(methyl methacrylate)–titania hybrid materials using allyl acetylacetone as a coupling agent. However, chelating ligands are normally retained, which alters the structure of the final network and affects the optical properties.[1,13] Although previous studies have shown the successful preparation of polymer–titania hybrid films,[4,6,11] thin film properties based on the common optical polymer, PMMA, have, as yet, not been fully explored.

In this study, a series of PMMA–titania hybrid thin films were prepared by an *in situ* sol–gel process combined with spin coating and a multi-step baking process, as shown in Fig. 1. The used acrylic monomers were MMA and 3-(trimethoxysilyl)propyl methacrylate (MSMA). The alkoxide monomer for the preparation of the titania segment was titanium *n*-butoxide. As shown in Fig. 1, the reaction mixture was pre-polymerized, and spin coated as a thin film before gelation. Then, it was baked at different temperatures to complete the polymerization. The structures, thermal properties, AFM morphology and variation of the refractive indices and extinction coefficients in the wavelength range 190–900 nm were examined for the resulting films in the present study. The effects of the titania content on the properties of the hybrid materials are discussed.

Experimental

Materials

Methyl methacrylate (MMA, 99.8%, TCI), 3-(trimethoxysilyl)propyl methacrylate (MSMA, 98%, Aldrich), tetrahydrofuran (THF, 99.9%, Acros) and ethyl alcohol (EtOH, 95%, Osaka) were purified by vacuum distillation. Titanium *n*-butoxide [$Ti(OBu)_4$, 99%, TCI], benzoyl peroxide (BPO, 98%, Shimakyu), and HCl (36%, Katayama) were used as received.

Preparation of hybrid polymer films

The compositions of the monomer mixtures for preparing polymer films are listed in Table 1. The monomers, MMA and MSMA, and the initiator, BPO, were added to a reaction flask and were polymerized at 60 °C under an N_2 flow for 2 h. Then, a homogeneous mixture of deionized water, hydrochloric acid, and $Ti(OBu)_4$ in THF was added dropwise into the reaction mixture. A slow addition rate of the pre-hydrolyzed solution in THF was required to avoid local non-homogeneity. The reaction was allowed to proceed at 60 °C for another 2 h, and then the solution was spin coated at 3000 rpm on a silicon wafer for 20 s. The coated film was then cured at 60 °C for 1 min, 100 °C for 1 min, and 150 °C for 2 h. The mole ratio of [MSMA] to ([MMA]+[MSMA]) was 0.25. The amounts of

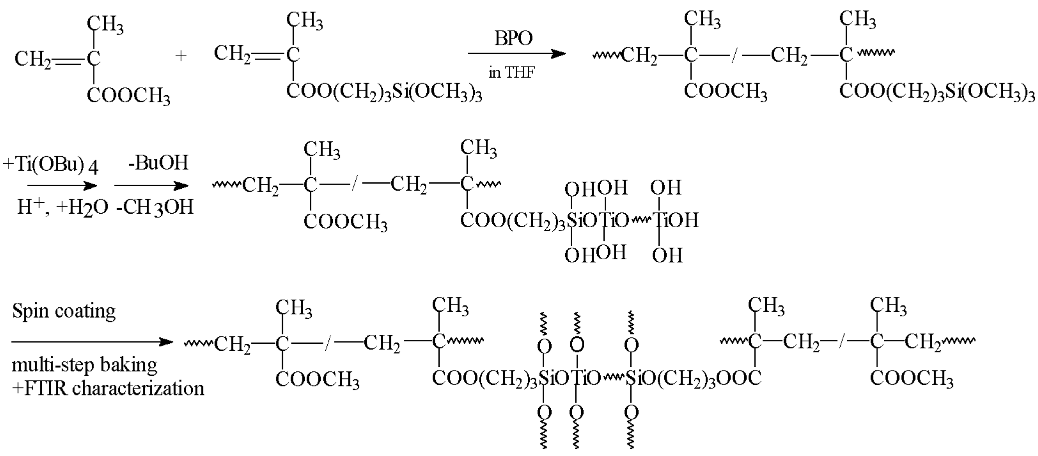

Fig. 1 Reaction scheme for the preparation of poly(methyl methacrylate)–titania hybrid polymer films.

HCl and deionized water were fixed at the following mole ratios: [HCl]/[Ti(OBu)$_4$] = 0.01 and [H_2O]/[Ti(OBu)$_4$] = 1.

Preparation of titania film

The preparation of the titania thin film was *via* a similar synthetic method to that reported in the literature.[14,15] The titania film was prepared by a sol–gel reaction according to the following reaction composition: (a) [HCl]/[Ti(OBu)$_4$] = 0.01, (b) [H_2O]/[Ti(OBu)$_4$] = 1, (c) [EtOH]/[Ti(OBu)$_4$] = 30. The reaction was performed at 60 °C for 2 h. Then, the reaction mixture was spin coated on a 6 in silicon wafer for 20 s. The coated film was then cured on a hot plate at 100 (1 min), 150 (1 min) and 250 °C (1 min), and finally cured in a furnace at 400 °C under a nitrogen atmosphere for 1 h.

Characterization

IR spectra of polymer thin films were taken from samples prepared by spin-coating the precursor solution on a KBr pellet, followed by curing at different temperature steps as described above, and were recorded at room temperature using a Jasco Model FTIR 410 spectrophotometer. Thermal analyses, thermogravimetric analysis (TGA) and differential scanning calorimetry (DSC) were performed under a nitrogen flow using a Dupont Model 951 thermogravimetric analyzer and a DuPont Model 910S differential scanning calorimeter at a heating rate of 20 and 10 °C min^{-1}, respectively. The TGA and DSC samples were prepared by spin-coating the precursor solution on a glass substrate, followed by curing at different temperature steps as described above. An *n*&*k* analyzer (n & k Technology, Inc.) was used to measure the refractive index (n) and the extinction coefficient (k) of the prepared films in the wavelength range 190–900 nm. The thickness (h) of the prepared films was also determined simultaneously. The abbe number (ν) of the prepared hybrid polymer film was calculated according to the following equation: $\nu = (n_D - 1)/(n_F - n_C)$, where n_C, n_D and n_F are the refractive indices of the polymer film at 656, 589 and 486 nm, respectively. An atomic force microscope (Digital Instrument, Inc., Model DI 5000 AFM) was used to probe the surface morphology of the coated films.

Table 1 Monomer mixtures (wt%) used to prepare hybrid films

	MMA	MSMA	Ti(OBu)$_4$
T0	54.7	45.3	—
T10	49.3	40.7	10
T20	43.8	36.2	20
T25	41.7	34.0	25
T33	36.7	30.3	33
T100	—	—	100

Results and discussion

Fig. 2 shows the FTIR spectra of the prepared poly(methyl methacrylate)–titania hybrid films **T0–T33**. Stretching vibration bands of the C–O–C or Si–O–Si, Si–C, C=O, C–H, and O–H bonds are observed at 1039–1192, 1267, 1730, 2950 and 3439–3504 cm^{-1}, respectively. The band at 914 cm^{-1} corresponds to the stretching vibration of the Ti–O–Si bond.[16] The Ti–O–Si band gradually increases in intensity with increasing titania content, which indicates a greater incorporation of titania into the PMMA network. The absorption band at 1524 cm^{-1} is probably due to the acrylate group bonded to titanium.[13] The positions of the above absorption bands are similar to those reported in the literature.[6,13,16] The Ti–OH band is observed at 3504, 3498, 3450, and 3439 cm^{-1} for **T10**, **T20**, **T25** and **T33**, respectively. The presence of Ti–OH groups may be due to the low curing temperature since a temperature of >400 °C is required for the synthesis of the inorganic TiO_2

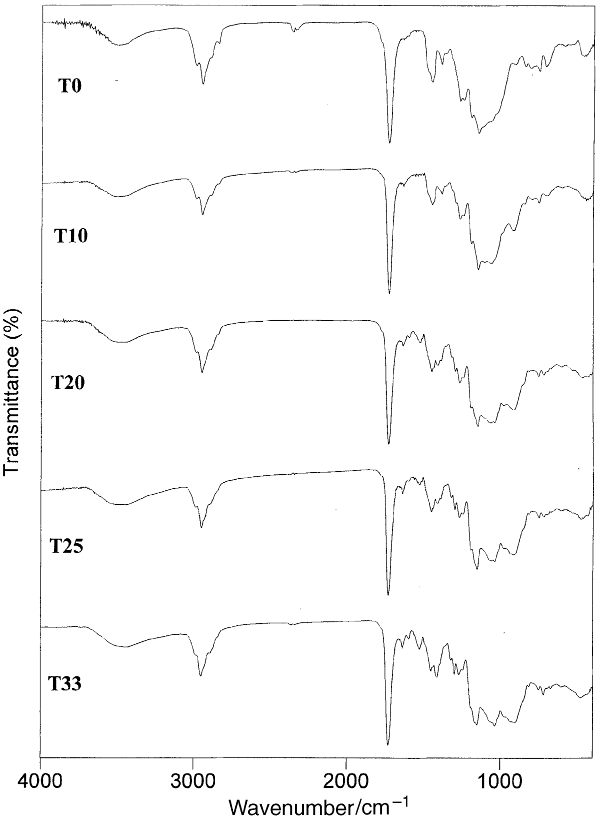

Fig. 2 FTIR spectra of poly(methyl methacrylate)–titania hybrid polymer films **T0–T33**.

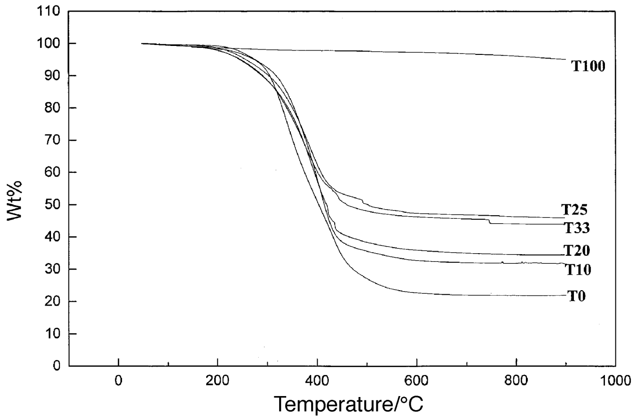

Fig. 3 TGA curves for **T0**, **T10**, **T20**, **T25**, **T33** and **T100** films at a heating rate of 20 °C min^{-1} under a nitrogen flow.

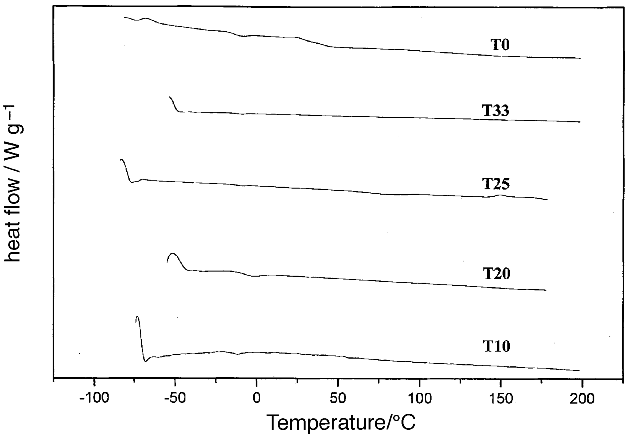

Fig. 4 DSC curves of **T0**, **T10**, **T20**, **T25** and **T33** films at a heating rate of 10 °C min^{-1} under a nitrogen flow.

materials. According to the literature,[17] the FTIR band of free hydroxy groups would lie in the range 3520–3600 cm^{-1}. Hence, the Ti–OH bonds observed here probably show hydrogen bonding with the carbonyl group of the MMA moiety. Although the Ti–OH group cannot be completely polymerized, hydrogen bonding of residual Ti–OH groups with carbonyl groups leads to the hybrid polymer film having high stability and high optical transparency.

Fig. 3 illustrates TGA curves for **T0**, **T10**, **T20**, **T25**, **T33** and **T100** films at a heating rate of 20 °C min^{-1} under a nitrogen flow. The titania film, **T100**, does not show any significant weight loss (<5 wt%) in the studied temperature range. The prepared hybrid polymer films have thermal decomposition temperatures of 277, 246, 258 and 248 °C for **T10**, **T20**, **T25** and **T33**, respectively. These values are similar to that of poly(MMA–MSMA) (**T0**). Decomposition is probably due to destruction of the PMMA segments because of the low bond dissociation energy of the C–C bond in the main chain. However, the char yields (polymer residues) of **T10–T33** at 900 °C are much larger than that of **T0**. The char yield generally increases with the titania content in the hybrid materials although those of **T25** and **T33** show no significant variation, as shown in Table 2. Furthermore, the experimental polymer residues at 900 °C are much larger than the calculated inorganic residues at 900 °C, which can be attributed to organic moieties trapped in the inorganic matrix. The black color of the char after TGA runs also indicates trapping of organic moieties in the inorganic matrix. The above results suggest that the thermal stability can be probably enhanced by using a larger quantity of the inorganic moiety (titania). Fig. 4 illustrates the DSC curves of **T0**, **T10**, **T20**, **T25** and **T33** at a heating rate of 10 °C min^{-1} under a nitrogen flow. Only poly(MMA–MSMA) (**T0**) shows a glass transition temperature (28.3 °C) suggesting that the inorganic moieties make the polymer chain segments immobile and thus probably raising the glass transition temperature to close to the decomposition temperature and hence their non-observation in the DSC curves. The DSC study also indicates good thermal stability of the prepared films with no phase separation occurring in the hybrid films.

Fig. 5 illustrates AFM images of (a) **T10** and (b) **T100**. The average roughness (R_a) and mean square roughness (R_q) of the hybrid film **T10** are 2.5 and 3.2 Å, respectively. By comparison, the thickness of the hybrid film **T10** is 10043 Å. Hence, the roughness of the hybrid film is $<0.1\%$ of the film thickness, which suggests a high degree of smoothness of the prepared film. The SEM diagram did not resolve any surface morphology of the **T10** film. These results suggest that the domain size of the TiO_2 segments in the **T10** structure is very small. In comparison, the titania film **T100** has higher ratio of roughness to thickness (*ca.* 0.5%) than the hybrid films **T0–T33**, as shown in Table 2. This result indicates that the TiO_2 particle size grows to a larger extent in the titania film and thus a higher degree surface roughness is observed [Fig. 5(b)]. The low roughness of the prepared hybrid films compared with their thicknesses suggests a very high degree of smoothness. Another possible explanation of the surface roughness results is in terms of the morphology, *i.e.*, the **T100** film is probably crystalline whereas the hybrid films are amorphous. A future study by X-ray diffraction will explore the morphology of the prepared films.

Fig. 6 shows the refractive index (n) distributions for **T0**, **T10**, **T20**, **T25** and **T33** films in the wavelength range 190–900 nm. The refractive index of the prepared hybrid films at 633 nm increases from 1.491 for **T0** to 1.553 for **T33** (Table 2). The refractive index of the titania film **T100** at 633 nm is 2.01, which is much larger than that of PMMA owing to the larger molar polarization of titania. Hence, the incorporation of titania segments into the PMMA matrix results in an increase of refractive index. The peak maximum in Fig. 6 results from the absorption of TiO_2 domains since the PMMA segment shows no absorption in the studied region. The abbe numbers (v) of the prepared hybrid films are in the range 30–49, which is much larger than for the titania film, **T100**. Since **T100** has an absorption edge in the visible region, this results in a larger difference of refractive index at the C-line (656 nm), D-line (589 nm) and F-line (486 nm) than for the hybrid films. The

Table 2 Properties of the prepared hybrid materials

Sample	T_d/°C	900 °C residue^a (wt%)	900 °C residue^b (wt%)	h^c/Å	$R_a{}^d$/Å	$R_q{}^d$/Å	n (633 nm)^e	v/^{f}
T0	257	24.9	10.9	5285	3.0	3.8	1.491	36.5
T10	277	31.7	13.4	10043	2.5	3.2	1.505	42.8
T20	246	34.5	16.5	2620	3.8	4.7	1.531	30.2
T25	258	45.9	18.2	5010	5.5	7.0	1.546	49.1
T33	248	44.0	21.3	3275	3.3	4.3	1.553	48.4
T100	—	95.1	100	604	2.5	3.2	2.01	14.2

[a] Experimental results from TGA. [b] Theoretical values based on the assumption that only inorganic moieties are present at 900 °C. [c] Film thickness. [d] R_a and R_q are average and mean square root roughness, respectively. [e] n = Refractive index. [f] v = Abbe number.

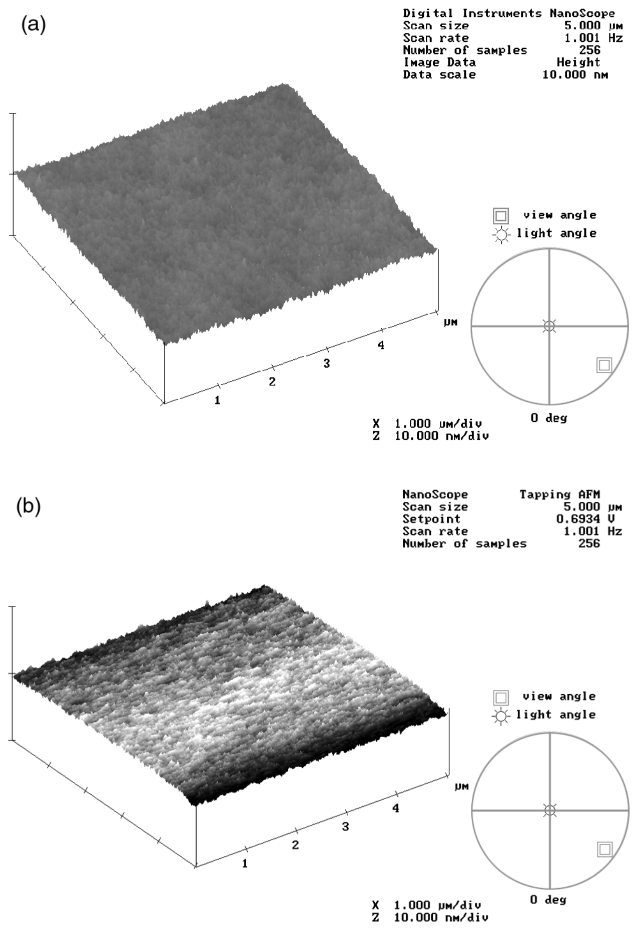

Fig. 5 AFM images of (a) **T10** and (b) **T100**; scan area is 5 × 5 µm.

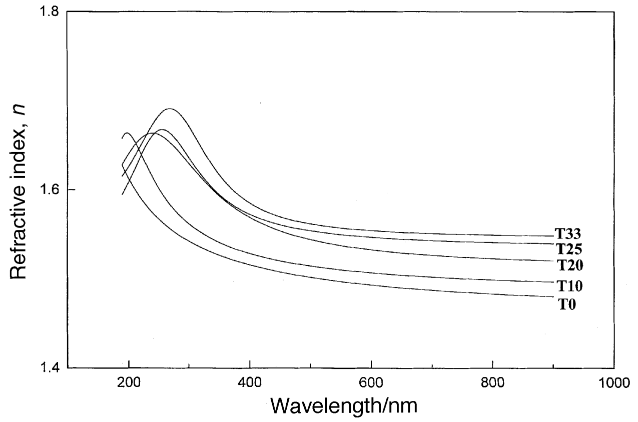

Fig. 6 Variation of the refractive indices (n) of the hybrid films **T0–T33** in the wavelength range 190–900 nm.

hybrid films have a small dispersion of refractive index in the visible region and large abbe numbers are obtained. This result can be also explained from the molecular structural point of view. Since the hybrid films do not have large continuous Ti–O–Ti segments as found for **T100**, the absorption edge is in the UV region and thus results in a large abbe number. For commercial applications, a minimum value of abbe number is 30 and so the prepared hybrid films are potentially useful. Fig. 7 illustrates the variation of the refractive index of the hybrid polymer films with different TiO_2 contents. The refractive index is proportional to the TiO_2 mole fraction in the range 0–0.166 and thus the refractive index can be tuned by this parameter. Fig. 8 shows the extinction coefficient (k) of **T0**, **T10**, **T20**, **T25** and **T33** films in the wavelength range 190–900 nm. The k values are almost zero for the studied films in the wavelength range 350–900 nm, which indicates their excellent optical transparency. Absorption in the wavelength range 190–350 nm is caused by electronic transitions of the Ti–O–Ti chains and the charge transfer effect of the Ti–O–Ti segment increases with its size.[18,19] Hence, the absorption maximum shows a red shift upon increasing the titania content. As reported in the literature,[18] the shift of the peak maximum becomes significant for a TiO_2 particle size <100 Å and the band edge of bulk TiO_2 with a particle size of 55 Å is 398 nm. Since the absorption band edges of the prepared hybrid films are in the range of 230–311 nm, this provides further evidence that the TiO_2 segments of the prepared hybrid films are very small. Table 2 lists the refractive indices, extinction coefficients and abbe numbers of the prepared films. These results suggest that the optical properties of the prepared hybrid films can be tuned by their molecular composition.

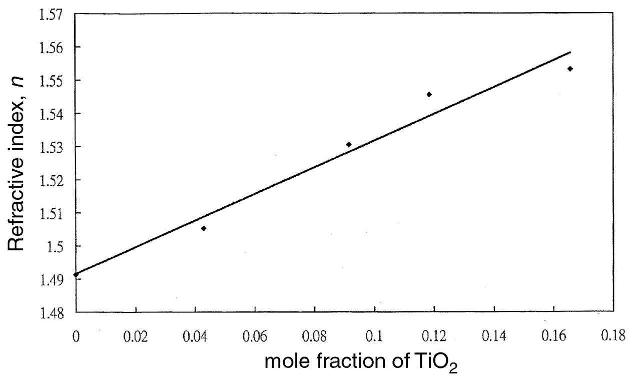

Fig. 7 Variation of refractive index with the mole ratio of titania in the hybrid material.

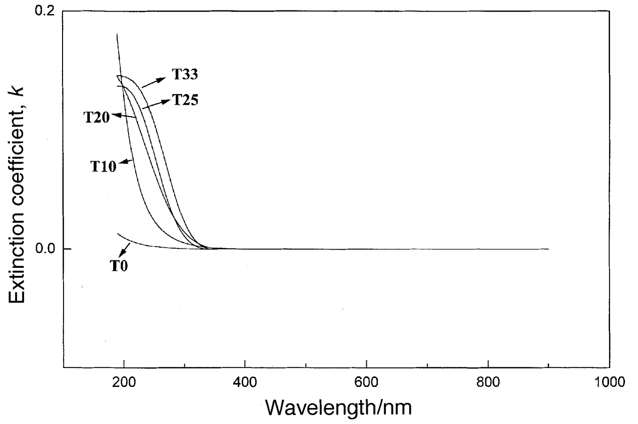

Fig. 8 Variation of the extinction coefficients (k) of the hybrid films **T0–T33** in the wavelength range 190–900 nm.

Conclusions

A series of PMMA–titania hybrid thin films have been successfully prepared by an *in situ* sol–gel process combined with spin coating and multi-step baking. DSC studies suggest a good dispersion of the PMMA segments in the titania network while AFM suggests that the prepared hybrid thin films are very flat. The refractive indices of the prepared hybrid thin films are proportional to the titania content. Excellent optical transparency in the visible region was observed for the prepared hybrid films. The shift of the absorption maximum of the prepared hybrid thin films can be correlated with the titania content and is increased with increased titania content. In summary, the prepared hybrid thin films are potentially useful as optical thin films.

Acknowledgements

We thank the National Science Council of Taiwan for financial support of this work under contract (NSC88-2214-E002-033). Financial support from the Union Chemical Lab. Of ITRI, Hsinchu, Taiwan, is also highly appreciated.

References

1 J. Wen and G. L. Wilkes, *Chem. Mater.*, 1996, **8**, 1667.
2 K. G. Sharp, *Adv. Mater.*, 1998, **10**, 1243.
3 G. Philipp and H. Schmidt, *J. Non-Cryst. Solids*, 1984, **63**, 283.
4 B. Wang, G. L. Wilkes, J. C. Hedrick, S. C. Liptak and J. E. McGrath, *Macromolecules*, 1991, **24**, 3449.
5 P. Papadimitrakopoulos, P. Wisniecki and D. Bhagwagar, *Chem. Mater.*, 1997, **9**, 2928.
6 M. Yoshida and P. N. Prasad, *Chem. Mater.*, 1996, **8**, 235.
7 A. Ershad-Langroudi, C. Mai, G. Vigier and R. Vassoille, *J. Appl. Polym. Sci.*, 1997, **65**, 2387.
8 H. Jiang and A. K. Kakkar, *Adv. Mater.*, 1998, **10**, 1093.
9 J. Biteau, F. Chaput, K. Lahlil, J. P. Boilot, G. M. Tsivgoulis, J. M. Lehn, B. Darracq, C. Marois and Y. Levy, *Chem. Mater.*, 1998, **10**, 1945.
10 G. Cartenuto, Y. S. Her and E. Matijevic, *Ind. Eng. Chem. Res.*, 1996, **35**, 2929.
11 B. Wang and G. L. Wilkes, *J. Polym. Sci. Polym. Chem.*, 1991, **29**, 905.
12 Z. H. Huang and K. Y. Qiu, *Polymer*, 1997, **38**, 521.
13 J. Zhang, S. Luo and L. Gui, *J. Mater. Sci.*, 1997, **32**, 1469.
14 B. Samuneva, V. Kozhukharov, Ch. Trapalis and R. Kranold, *J. Mater. Sci.*, 1993, **28**, 2353.
15 V. Kozhukharov, Ch. Trapalis and B. Samuneva, *J. Mater. Sci.*, 1993, **28**, 1283.
16 A. Leaustic, F. Babonneau and J. Livage, *Chem. Mater.*, 1989, **1**, 240.
17 B. K. Coltrain, C. J. T. Landry, J. M. O'Reilly, A. M. Chamberlain, G. A. Rakes, J. S. Sedita, L. W. Kelts, M. R. Landry and V. K. Long, *Chem. Mater.*, 1993, **5**, 1445.
18 M. Anpo, T. Shima, S. Kodama and Y. Kubokawa, *J. Phys. Chem.*, 1987, **91**, 4305.
19 H. Yoneyama, S. Haga and S. Yamanaka, *J. Phys. Chem.*, 1987, **93**, 4833.

Paper 9/06157F